ResearchGate

See discussions, stats, and author profiles for this publication at: https://www.researchgate.net/publication/228469028

Self-Assembled Monolayers of Methyl 1-Thiahexa(ethylene oxide) for the Inhibition of Protein Adsorption

ARTICLE *in* LANGMUIR · JUNE 2002

Impact Factor: 4.46 · DOI: 10.1021/la025720t

CITATIONS
69

READS
25

3 AUTHORS:

David J Vanderah
Institute for Bioscience and Biotechnology R…
90 PUBLICATIONS **1,825** CITATIONS
SEE PROFILE

Gintaras Valincius
Vilnius University
82 PUBLICATIONS **1,085** CITATIONS
SEE PROFILE

Curtis W Meuse
National Institute of Standards and Technolo…
64 PUBLICATIONS **1,307** CITATIONS
SEE PROFILE

Available from: David J Vanderah
Retrieved on: 26 January 2016

Self-Assembled Monolayers of Methyl 1-Thiahexa(ethylene oxide) for the Inhibition of Protein Adsorption

David J. Vanderah,*,[1] Gintaras Valincius,[†] and Curtis W. Meuse*,[1]

Biotechnology Division, National Institute of Standards and Technology, 100 Bureau Drive, Stop 8313, Gaithersburg, Maryland 20899-8313

Received March 11, 2002

Self-assembled monolayers (SAMs) of methyl 1-thiahexa(ethylene oxide), $HS(CH_2CH_2O)_6CH_3$, on gold with different molecular conformations were evaluated for their ability to inhibit protein adsorption. Assembled from 95% ethanol, reflection−absorption infrared spectroscopy (RAIRS) data show that the $HS(CH_2CH_2O)_6CH_3$ SAMs adopt the well-ordered 7/2 helical conformation of the folded-chain crystal polymorph of poly(ethylene oxide). Electrochemical impedance spectroscopy (EIS) data indicate that these ordered helical SAMs behave as near ideal capacitors in an electrochemical environment. Assembled from other solvents, the SAMs of $HS(CH_2CH_2O)_6CH_3$ were more variable and less ordered. For samples assembled from 100% ethanol, the RAIRS data were virtually identical to those obtained from 95% ethanol indicating the predominant 7/2 helical structure but the EIS spectra show consistently higher specific capacitance values indicating a slight increase in disorder or number of defect sites. In contrast to the ethanolic solvents, assembled from tetrahydrofuran, the $HS(CH_2CH_2O)_6CH_3$ SAMs are significantly less ordered with RAIRS data clearly showing mixtures of the 7/2 helical and nonhelical conformations and EIS data showing much higher specific capacitance values. Exposure of these ordered and disordered $HS(CH_2CH_2O)_6CH_3$ SAMs to bovine serum albumin and lysozyme solutions showed that the less ordered SAMs exhibit better inhibition of protein adsorption.

Introduction

Surfaces that expose ethylene oxide (EO) segments, that is, $(CH_2CH_2O)_x$, to biological fluids or tissues have been actively investigated for biomedical applications.[2−4] The biocompatibility of these surfaces is largely attributed to their decreased adsorption of blood proteins.[5] A number of theories have been advanced to account for the protein resistance of poly(ethylene oxide) [PEO]. These include steric repulsion, large PEO exclusion volume, rapid mobility of highly hydrated PEO chains, low PEO−water interfacial energy, and weak PEO−protein binding interactions.[6]

More recently, the self-assembled monolayers (SAMs) of ω-oligo(ethylene oxide) [OEO] alkanethiols, **1a**−**1c**, have been found to be highly protein resistant.[7−16] Initial studies,[11] which compared the mechanism of protein adsorption of these SAMs, with short OEO segments, to that of PEO and related PEO copolymers, framed their efforts in terms of the steric repulsion model.[17,18] The steric repulsion hypothesis attributes the protein resistance of EO segments to steric effects that oppose the EO−protein surface attractive forces (hydrophobic and van der Waals). This steric repulsion has elastic and osmotic components. The elastic component is caused by the compression and restriction of the EO chains/segments. The osmotic component is caused by the loss of "waters of hydration" from both the EO chains/segments and the protein. Because the more densely packed, shorter ω-OEO SAMs have less conformational freedom to lose, upon protein adsorption, than the less densely packed, longer PEO

$$M(CH_2CH_2O)_xR$$

1

1a: x = 1 - 7 and ~ 17, M = $HS(CH_2)_{11}O$ and R = H or CH_3[7,9,11,14-16]
1b: x = 3, M = $HS(CH_2)_{11}CH(CH_2OCH_3)CH_2O$ and R = CH_3[11]
1c: x = 3 - 6, M = $HS(CH_2)_{11}CONH$ and R = H or CH_3[10]

* To whom correspondence should be addressed.
[†] NIST Guest Researcher, Biotechnology Division. Permanent address: Institute of Biochemistry, Mokslininku 12, Vilnius 2600, Lithuania.
(1) E-mail: david.vanderah@nist.gov; curtis.meuse@nist.gov.

(2) *Poly(ethylene Glycol) Chemistry*: *Biotechnical and Biomedical Applications*; Harris, J. M., Ed.; Plenum Press: New York, 1992.
(3) Bailey, F. E., Jr.; Koleske, J. Y. *Poly(ethylene Oxide)*; Academic Press: New York, 1984.
(4) Lasic, D. D.; Martin, F. *Stealth Liposomes*; CRC Press: Boca Raton, FL, 1995.
(5) Nogaoka, S.; Mori, Y.; Takiuchi, H.; Yokota, K.; Tanizawa, H.; Nishiumi, S. In *Polymers as Biomaterials*; Shalaby, S., Hoffman, A., Ratner, B. D., Horbett, T. A., Eds.; Plenum Press: New York, 1984; pp 361−374.
(6) Gombatz, W. R.; Guanghui, W.; Horbett, T. A.; Hoffman, A. S. *Poly(ethylene Glycol) Chemistry*: *Biotechnical and Biomedical Application*; Harris, J. M., Ed.; Plenum Press: New York, 1992; pp 247−261 and all references therein.
(7) Zolk, M.; Eisert, F.; Pipper, J.; Herrwerth, S.; Eck, W.; Buck, M.; Grunze, M. *Langmuir* **2000**, *16*, 5849−5852.
(8) Chapman, R. G.; Ostuni, E.; Yan, L.; Whitesides, G. M. *Langmuir* **2000**, *16*, 6927−6936.
(9) Feldman, K.; Hähner, G.; Spencer, N. D.; Harder, P.; Grunze, M. *J. Am. Chem. Soc.* **1999**, *121*, 10134−10141.
(10) Benesch, J.; Svedhem, S.; Svensson, S. C. T.; Valiokas, R.; Liedberg, B.; Tengvall, P. *J. Biomater. Sci., Polym. Ed.* **2001**, *12*, 581−597.
(11) Harder, P.; Grunze, M.; Dahint, R.; Whitesides, G. M.; Laibinis, P. E. *J. Phys. Chem. B.* **1998**, *102*, 426−436.
(12) Mrksich, M.; Whitesides, G. M. *Using Self-Assembled Monolayers that Present Oligo(ethylene oxide) Groups to Control the Interactions of Proteins with Surfaces*, 1st ed.; Harris, J. M., Zalipsky, S., Eds.; American Chemical Society: Washington, DC, 1997; Vol. 680, pp 361−373 and references therein.
(13) Silin, V.; Weetall, H.; Vanderah, D. J. *J. Colloid Interface Sci.* **1997**, *185*, 94−103.
(14) Prime, K. L.; Whitesides, G. M. *J. Am. Chem. Soc.* **1993**, *115*, 10714−10721.
(15) Prime, K. L.; Whitesides, G. M. *Science* **1991**, *252*, 1164−1167.
(16) Pale-Grosdemange, C.; Simon, E. S.; Prime, K. L.; Whitesides, G. M. *J. Am. Chem. Soc* **1991**, *113*, 12−20.
(17) Jeon, S. I.; Lee, J. H.; Andrade, J. D.; De Gennes, P. G. *J. Colloid Interface Sci.* **1991**, *142*, 149−158.
(18) Jeon, S. I.; Andrade, J. D. *J. Colloid Interface Sci.* **1991**, *142*, 159−166.

10.1021/la025720t This article not subject to U.S. Copyright. Published 2002 by the American Chemical Society
Published on Web 05/11/2002

chains, their protein resistance was generally attributed to the osmotic component of the steric repulsion model.[7,11]

To test this hypothesis, the protein resistances of SAMs with different OEO segment compositions and conformations were compared.[11] On gold, reflection−absorption infrared spectroscopy (RAIRS) data indicated the OEO segments of **1a** SAMs ($x = 3$ and 6) to be mixtures of "crystalline helical and amorphous" conformations. On silver, RAIRS data indicated that the OEO segments were largely in an all-trans conformation. Protein adsorption experiments with these surfaces revealed that only the **1a** SAMs ($x = 3$), on silver, adsorbed protein. All SAMs with other compositions and conformations, on gold, were highly protein resistant.[11]

The differences between the protein resistances of the **1a** SAMs ($x = 3$) on silver and gold were further investigated using ab initio calculations,[19,20] scanning force microscopy,[9] vibrational sum frequency spectroscopy,[7] and grand canonical Monte Carlo techniques.[21] These studies generally support the hypothesis that protein resistance is due to the presence of a tightly bound water layer at the surface of helical or mixed helical and amorphous OEO segments on gold substrates. They suggest that the density of hydrogen bonds between the water layer and helical OEO segments on gold, with nearest-neighbor lateral distances of ∼0.50 nm,[20] may be higher than that at the surface of all-trans OEO segments on silver, with smaller nearest-neighbor lateral distances (∼0.44 nm[20]). Alternatively, a study using scanning force microscopy suggests that the protein resistance may be due to a "unique" set of repulsive forces of OEO segments on gold.[9] This study observed a strong dependence of repulsive forces on the solution ionic strength that suggested the protein resistance of OEO segments may be related to repulsive electrostatic interactions that are stronger for the protein-resistant SAMs on gold than for the protein-adsorbent SAMs on silver.

The impetus for this study was derived from our characterization of the SAMs of $HS(CH_2CH_2O)_xR$, where $x = 4-8$ and $R = C_{10}H_{21}$ or $C_{18}H_{37}$.[22,23] For $x = 6$, RAIRS data indicated highly ordered SAMs in which the 1-thiahexa(ethylene oxide) [THEO] segment exists in a 7/2 helical conformation, hereafter referred to as the helix or the helical conformation. The four bands in the RAIRS spectra in the 1400−900 cm^{-1} region at 1345, 1243, 1118, and 966 cm^{-1}, which correspond to those vibrations with transition moments parallel to the chain axis, matched the symmetry designated A_2 (4) to A_2 (7) bands, respectively, for the folded-chain crystal (FCC) polymorph of crystalline PEO.[24] The THEO segment is oriented normal to the substrate because of a nearly perfect match between the cross-sectional area of the helix, 21.38 $Å^2$, and the packing density, 21.4 $Å^2$/thiolate,[25] of a $(\sqrt{3} \times \sqrt{3})R30°$ adlayer on Au [assuming predominantly (111) Au with S ··· S ≅ 0.50 nm]. With the helix normal to the substrate, the oxygen atoms in each of the EO units of the THEO segment are co-located in planes, here parallel to the substrate, as are the oxygen atoms in each of the EO units in the unit cell of the FCC polymorph of PEO (planes normal to the c axis of the unit cell).[23] Similar SAM structures for C_{10} and C_{18} suggested that the structure of the THEO segment may be independent of the length of the alkyl group. Thus, $HS(CH_2CH_2O)_6CH_3$, **1d**, might be expected to form conformationally well-defined, helical, OEO SAMs that are well suited for protein adsorption studies. This paper reports the preparation, the characterization, and the protein adsorption properties of this system.

Scheme 1. Synthesis of $HS(CH_2CH_2O)_6CH_3$[a]

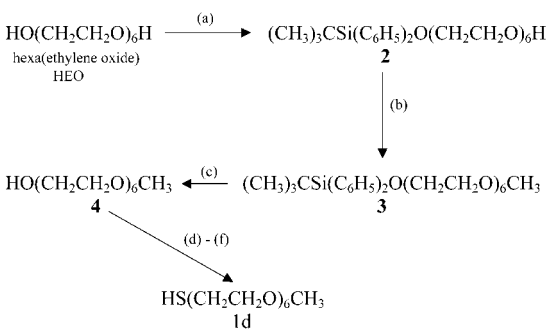

[a] (a) *tert*-Butyldiphenylsilyl chloride/imidazole−DMF, RT, 1 h; (b) NaH/THF, 0 °C to RT, then CH_3I/THF, reflux, 1 h; (c) (n-butyl)$_4$ammonium fluoride/H_2O−THF, RT, 2 h; (d) trifluoroacetic anhydride, RT, 1 h, remove volatiles, then LiBr/THF−HMPA, reflux, 18 h; (e) 2 equiv CH_3COSH/MeOH; (f) 0.1 N HCl/MeOH, reflux, 4 h.

Materials and Methods[26]

Synthesis. All chemicals, except tetrahydrofuran (THF), were purchased from Aldrich Chemical Co. (Milwaukee, WI). THF (Mallinckrodt AR) was purchased from North Strong Scientific (Phillipsburg, NJ). THF and hexamethylphosphoramide (HMPA) were distilled from calcium hydride. The THF was distilled under N_2 immediately before use, whereas the HMPA was distilled and stored under N_2 over 0.3 nm molecular sieves. All solvents used in the preparation of the 0.5 mM thiol solutions were distilled. The 100% ethanol solution was prepared by distilling 99.5% ethanol from sodium under dry N_2. Bovine serum albumin (BSA) and lysozyme were purchased from Sigma Chemical Co., St. Louis, MO.

The synthesis of $HS(CH_2CH_2O)_6CH_3$, **1d**, is outlined in Scheme 1. Hexa(ethylene oxide) [HEO] was protected as a mono-*tert*-butyldiphenylsilyl ether, **2**. The remaining hydroxyl group was then methylated by standard procedures to give **3** followed by removal of the silyl protecting group to give **4**. Finally, **4** was converted to methyl 1-thiahexa(ethylene oxide),[27] **1d**, by known methods.[16] Structural assignments for **2**−**4** were made from proton nuclear magnetic resonance (^{1}H NMR) spectroscopy and low-resolution mass spectroscopy (MS) data. All compounds were purified by flash chromatography (silica gel) to single spots by thin-layer chromatography (>98% purity). The structural assignment of **1d** was made from ^{1}H NMR and high-resolution mass spectrometry data.[28]

Sample Preparation. Silicon (100) wafers (Virginia Semiconductor, Fredricksburg, VA) were coated initially with chromium (∼2 nm) and then with gold (∼200 nm) by magnetron sputtering (Edwards Auto 306, U.K.) at a base pressure of ∼1.3 × 10^{-6} mbar as described previously.[23] Substrates were found

(19) Pertsin, A. J.; Grunze, M.; Garbuzova, I. A. *J. Phys. Chem. B* **1998**, *102*, 4918−4926.
(20) Wang, R. L. C.; Kreuzer, H. J.; Grunze, M. *J. Phys. Chem. B* **1997**, *101*, 9767−9773.
(21) Pertsin, A. J.; Grunze, M. *Langmuir* **2000**, *16*, 8829−8841.
(22) Vanderah, D. J.; Pham, C. P.; Springer, S. K.; Silin, V.; Meuse, C. W. *Langmuir* **2000**, *16*, 6527−6532.
(23) Vanderah, D. J.; Meuse, C. W.; Silin, V.; Plant, A. L. *Langmuir* **1998**, *14*, 6916−6923.
(24) Kobayashi, M.; Sakashita, M. *J. Chem. Phys.* **1992**, *96*, 748−760.
(25) Laibinis, P.; Bain, C. D.; Nuzzo, R. G.; Whitesides, G. M. *J. Phys. Chem.* **1995**, *99*, 7663−7676.

(26) The specification of commercial products is for clarity only and does not constitute endorsement by NIST.

(27) IUPAC name: 3,6,9,12,15,18-hexaoxanonadecanethiol.

(28) 270 MHz ^{1}H NMR: δ 3.7−3.54 [22H, br. s, $CH_3(OCH_2CH_2)_5CH_2CH_2SH$], 3.38 (3H, s, CH_3O−), 2.70 (2H, q, $J = 6$ Hz, $-OCH_2CH_2SH$), 1.60 (1H, t, $J = 6$ Hz, $-CH_2SH$). Fast atom bombardment high-resolution mass spectrometry (FAB HRMS): $[M + H]^+$ ($C_{13}H_{29}O_6S$) calcd, 313.1793; found, 313.1684. The MS also showed disulfide $[C_{13}H_{29}O_6S]_2$ at m/z = 622.3, which was not seen in the ^{1}H NMR spectrum, indicating that it may have formed in the MS ionization process.

to be smooth (root-mean-square of ~0.3 nm at 10 nm thickness and ~1 nm at 200 nm thickness) and contained relatively few defects as indicated by earlier impedance measurements[29] and neutron reflectivity studies[30] on SAMs of $HS(CH_2CH_2O)_6C_{18}H_{37}$. The monolayers for this study were prepared by immersing the gold substrates in $\sim 0.5 \times 10^{-3}$ mol/L solutions of $HS(CH_2CH_2O)_6CH_3$ for at least 3 days in one of three different solvents: THF, 100% ethanol, or 95% ethanol.

Visible Spectroscopic Ellipsometry (SE). Multiple wavelength ellipsometric measurements were performed on a J. A. Woollam Co., Inc. (Lincoln, NE) M-44 spectroscopic ellipsometer aligned at a nominal incidence angle of ~70° from the surface normal [the exact incidence angle, which varied slightly from day to day, was determined by the modeling software (WVASE)]. Prior to the SE measurements, the samples were removed from the thiol solution, rinsed with the corresponding solvent, and then dried in a stream of dry N_2. Four measurements were obtained for each sample, and to reduce noise, 3000 revolutions of the analyzer were accumulated. Thicknesses were calculated relative to the thickness of the SAM of $(C_{18}D_{37}S)_2$ on Au. The optical constants of the gold were determined using a two-layer model for a SAM of $(C_{18}D_{37}S)_2$ for which we assumed a thickness of 2.3 nm and a refractive index of 1.45. The optical constants for the Au were then used to determine the thicknesses of the SAMs, assuming a refractive index of 1.45 for all compounds. Modeling and thickness calculations were carried out using the WVASE software from J. A. Woollam Co.

RAIRS Measurements. The RAIRS data were obtained using a Bruker Equinox 55 spectrometer (Billerica, MA) with an 80° external reflection accessory (International Crystal Laboratories, Garfield, NJ) and a germanium double diamond polarizer (Harrick Scientific, Ossing, NY). Prior to the RAIRS measurements, the monolayer samples were thoroughly rinsed with the corresponding solvent and then dried in a stream of dry N_2. Two scans (4 cm^{-1} resolution, 5 min each) were acquired both with and without the layer of interest. The Fourier transform was calculated after two levels of zero filling (Bruker Opus software). The spectrum of the sample was created from the average of the two scans (sample compared to background). A spectrum of the water vapor was produced from the average of the spectra created by comparing the sample versus sample and the background versus background scans. Spectral subtraction to remove the water vapor contributions was performed using Grams 32 software (Galactic Industries, Salem, NH). The spectral subtraction process is not perfect and can leave residual baseline noise due to extra water vapor from the samples just removed from the aqueous protein solutions. The final spectra were plotted using Origin (Microcal, Northampton, MA).

Protein Adsorption Experiments. Protein adsorption experiments largely followed a previously reported protocol.[14] All protein solutions were prepared with 10 mM phosphate buffer, pH = 7.5 (hereafter referred to as buffer). Final protein concentrations were 1 mg/mL for both BSA and lysozyme, which corresponds to 1.5×10^{-5} and 6.8×10^{-5} mol/L, respectively. After initial RAIRS analysis, the samples were cut into two pieces and immersed in 9.0 mL of buffer for 15 min to prewet the SAM surfaces. Protein was then added [1.0 mL of a protein stock solution (10 mg/mL)] and gently mixed. After 2 h, the samples were removed from the solution, rinsed first with buffer and then with water, and then dried in a stream of dry N_2 and immediately placed in the sample chamber for RAIRS measurements.

Contact Angle Measurements. Contact angles were determined with a Ramé-Hart model 110-00-115 goniometer at room temperature and ambient relative humidity (40° ± 5°) using water as the probing liquid. Contact angles (θ) were measured by lowering a 2−3 μL drop onto the surface from a blunt-ended needle attached to a 2 mL syringe. The contact angle was recorded immediately after the drop detached from the needle tip. The value of θ was the average of at least four measurements.

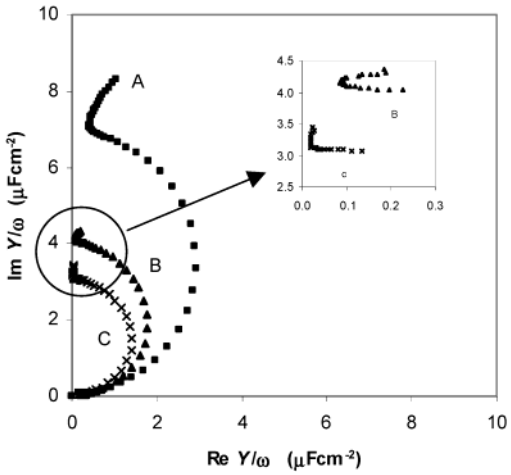

Figure 1. Complex capacitance plots of $HS(CH_2CH_2O)_6CH_3$ SAMs assembled from different solutions: A, THF; B, 100% ethanol; and C, 95% ethanol. The spectra cover the frequency range from 0.5 to 65 000 Hz. The figure inset displays the low-frequency range of spectra B and C.

Electrochemical Impedance Spectroscopy Measurements (EIS). The EIS measurements were obtained using a Solartron electrochemical impedance system (model 1286 potentiostat, model 1250 frequency response analyzer, computer, and software) (Farnborough, U.K.). A Pt spiral wire with a surface area of approximately 1 cm^2 and $Ag/AgCl/KCl_{sat}$ were used as the auxiliary and reference electrodes, respectively. All measurements were carried out at 0 V bias versus the reference electrode at 21 ± 1° C in 100 mM potassium phosphate buffer solutions containing 200 mM KCl. The EIS spectra were obtained for frequencies between 0.5 and 65 000 Hz with five measurements per decade and are presented in the complex capacitance form, that is, the plots of Im Y/ω versus Re Y/ω, where Y is the admittance and ω is the angular frequency [$\omega = 2\pi f$, and f is the frequency in hertz (Hz)]. The EIS data were fitted with ZView software (Scribner Associates). Simple models of the interface can be readily inferred when the electrochemical response exhibits capacitive behavior.

Results

SAMs of $HS(CH_2CH_2O)_6CH_3$ were prepared using three separate solvents: THF, 100% ethanol, and 95% ethanol. Solvent selection afforded a comparison of SAM formation from a nonhydroxylic (THF) and a hydroxylic solvent (100% ethanol), while 95% ethanol was selected to discern the effect, if any, of SAM formation in the presence of water (~5%). Film uniformity and defects of the $HS(CH_2CH_2O)_6CH_3$ SAMs were assessed using EIS measurements in an aqueous electrolyte environment. The complex capacitance spectra obtained from the $HS(CH_2CH_2O)_6CH_3$ SAMs assembled from THF (A), 100% ethanol (B), and 95% ethanol (C) are shown in Figure 1. Spectrum C is nearly perfectly semicircular over the frequency range between 0.5 and 65 000 Hz, indicating a highly uniform dielectric layer. Spectrum B is similar to spectrum C but differs at the very low end of the frequency range, which can be seen in the Figure 1 inset. Spectrum A exhibits a slightly suppressed semicircular shape with clear deviation from the semicircular form at the low end of the frequency range. These differences will be elaborated on more fully in the discussion section.

Figures 2 and 3 show the RAIRS spectra of the $HS(CH_2CH_2O)_6CH_3$ SAMs from THF (A), 100% ethanol (B), and 95% ethanol (C) between the regions from 1800 to 900 cm^{-1} and from 3100 to 2700 cm^{-1}, respectively. The absorption bands at 1346, 1242, 1118, and 964 cm^{-1} in the spectra from the ethanolic solvents (spectra B and C,

(29) Glazier, S. A.; Vanderah, D. J.; Plant, A. L.; Bayley, H.; Valincius, G.; Kasianowicz, J. J. *Langmuir* **2000**, *16*, 10428−10435.
(30) Majkrzak, C. F.; Krueger, S.; Dura, J.; Tarek, M.; Tobias, D.; Silin, V.; Meuse, C. W.; Woodward, J. T., IV; Plant, A. L. *Biophys. J.* **2000**, *79*, 3330−3337.

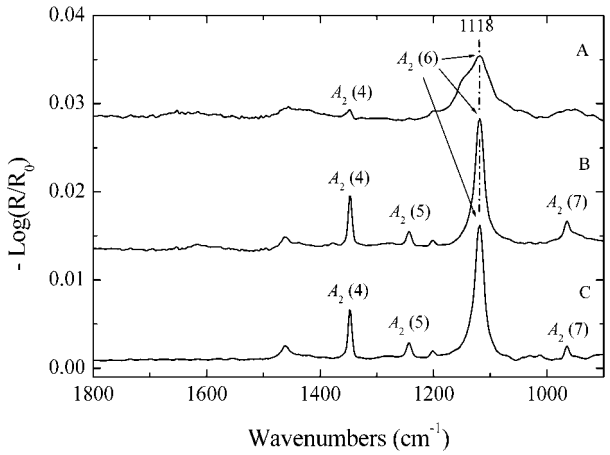

Figure 2. RAIRS spectra of $HS(CH_2CH_2O)_6CH_3$ from 1800 to 900 cm^{-1}: spectrum A from THF, spectrum B from 100% ethanol, and spectrum C from 95% ethanol. The spectra are offset for clarity.

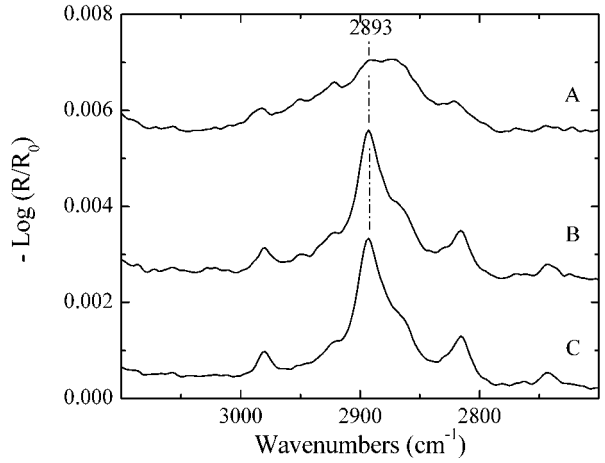

Figure 3. RAIRS spectra of $HS(CH_2CH_2O)_6CH_3$ from 3100 to 2700 cm^{-1}: spectrum A from THF, spectrum B from 100% ethanol, and spectrum C from 95% ethanol. The spectra are offset for clarity.

Figure 2), which correspond to those vibrations with transition moments parallel to the chain axis, are assigned as the symmetry designated A_2 (4) to A_2 (7) absorption bands, respectively, of the helical conformation of the FCC polymorph of PEO.[24] These band positions are essentially identical to the corresponding A_2 bands obtained for the longer alkyl chain compounds (R = $C_{10}H_{21}$ or $C_{18}H_{37}$)[23] indicating that the $HS(CH_2CH_2O)_6CH_3$ SAMs are in the helical conformation as illustrated in Figure 4. The only differences in this region between the $HS(CH_2CH_2O)_6CH_3$ SAMs and the SAMs of the longer alkyl chain compounds are the weak absorption band at 1206 cm^{-1}, assigned as an OCH_3 rocking mode,[11] and a narrower full width at half-maximum (fwhm) of the strong A_2 (6) band at 1118 cm^{-1}. The helical conformation present in the SAMs from the ethanolic solvents is also indicated by the prominent 2893 cm^{-1} band in the 3100−2700 cm^{-1} region (spectra B and C, Figure 3).[31]

The structures of the $HS(CH_2CH_2O)_6CH_3$ SAMs assembled from THF are distinctly different (spectra A, Figures 2 and 3) than the SAMs obtained from the ethanolic solvents. Figure 2 shows that the bands for the helical conformation are attenuated and show a larger

(31) Miyazawa, T.; Fukushima, K.; Ideguchi, Y. *J. Chem. Phys.* **1962**, *37*, 2764−2776.

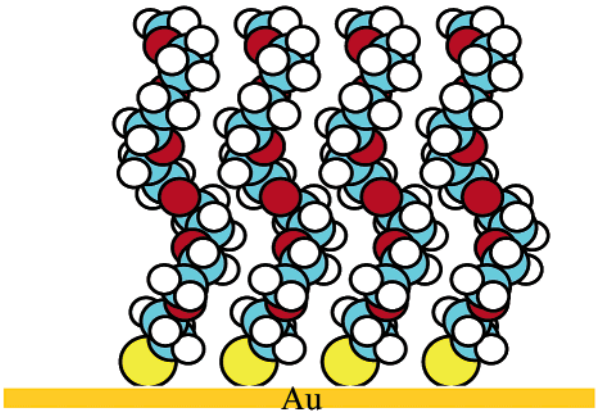

Figure 4. Schematic illustration of the $HS(CH_2CH_2O)_6CH_3$ SAM structure from ethanolic solvents on Au. Sphere color code = type of atom: blue = carbon; red = oxygen; yellow = sulfur; white = hydrogen.

fwhm for the A_2 (6) band (1118 cm^{-1}) than that for the A_2 (6) band for the SAMs from the ethanolic solvents. Additional spectral bands are also present, the most apparent of which is the high-frequency shoulder (∼1140 cm^{-1}) of the A_2 (6) band. Spectrum A (Figure 3) shows the attenuation of the band at 2893 cm^{-1} and the broadening of all the bands in the C−H stretching region. These data correlate with less ordered OEO conformations[11,22,32] and suggest that less ordered SAMs consisting of mixtures of helical and nonhelical conformations were obtained.

SE measurements of the $HS(CH_2CH_2O)_6CH_3$ SAMs deposited from 95% and 100% ethanol gave calculated thicknesses of 1.96 nm (±0.07 nm). This is in excellent agreement with an expected thickness of 1.99 nm for the $HS(CH_2CH_2O)_6CH_3$ SAMs in the helical conformation.[33] Contact angle measurements of these SAMs were $\theta = 70° \pm 2°$. The SAMs assembled from THF had variable SE film thicknesses and contact angle values (d = 1.0−1.8 nm and $\theta < 60°$, respectively), as well as higher and variable specific capacitance values (>4.5 $\mu F/cm^2$), as estimated from the EIS spectra. Deviation from the ethanolic solvents SE and contact angle values largely correlated with the amount of nonhelical conformations in the RAIRS spectra (data not shown).

Figures 5−7 show the RAIRS data obtained after 2 h of exposure to the BSA or lysozyme solutions for the SAMs assembled from 95% ethanol, THF, and 100% ethanol, respectively.[34] In each figure, the results from the BSA and the lysozyme solutions are spectra B and C, respectively. For direct comparison, Figures 5−7 include the RAIRS data of the SAMs before exposure to proteins (spectra A). Adsorbed BSA or lysozyme is indicated in the 1700−1500 cm^{-1} region by the presence of amide I and

(32) Dissanayake, M. A. K. L.; Frech, R. *Macromolecules* **1995**, *28*, 5312−5319.

(33) Film thickness calculation for $HS(CH_2CH_2O)_6CH_3$ SAMs: Helical conformation = 1.99 nm {1.67 nm [6/7 × 1.95 nm (*c* axis of PEO unit cell: Takahashi, Y.; Tadokoro, H. *Macromolecules* **1973**, *23*, 672−675)] + 0.04 nm (C−S bond length increase relative to a C−O bond) + 0.19 nm (Au−S bond length) + 0.09 nm {the methyl group = 1/3 of the thickness of one $-CH_2CH_2O-$ unit (0.278 nm)}. The S−Au bond distance from: Sellers, H.; Ulman, A.; Shnidman, Y.; Eilers, J. E. *J. Am. Chem. Soc.* **1993**, *115*, 9389−9401. All-trans extended conformation = 2.49 nm {2.14 (6 × 0.356 nm (ref 11)) + 0.04 nm (C−S bond length differential relative to C−O bond length) + 0.19 nm (Au−S bond length) + 0.12 nm (1/3 of 0.356 nm)}.

(34) The shift of the region from 1800−900 to 1800−1000 cm^{-1} in the figures after exposure to the protein solution emphasizes the region from 1700 to 1500 cm^{-1} where the amide I and amide II bands of the adsorbed protein are expected. Changes in the smallest A_2 band at 964 cm^{-1}, no longer shown, are difficult to see due to baseline deviations but generally followed those of the other A_2 bands.

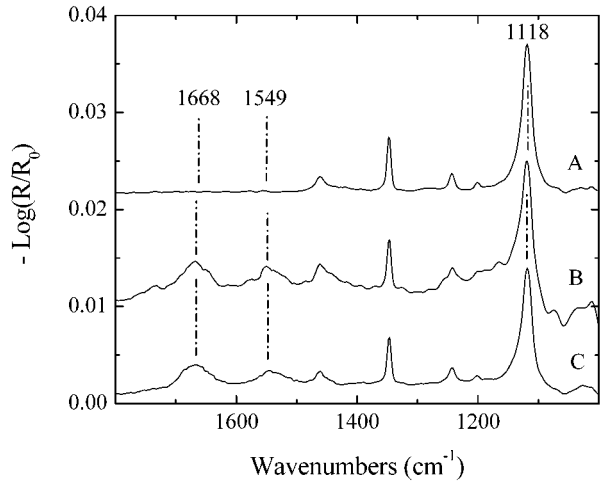

Figure 5. RAIRS spectra of the $HS(CH_2CH_2O)_6CH_3$ SAM from 1800 to 1000 cm^{-1} assembled from 95% ethanol: spectrum A, before exposure to protein solutions; spectrum B, after exposure to BSA; spectrum C, after exposure to lysozyme. The spectra are offset for clarity.

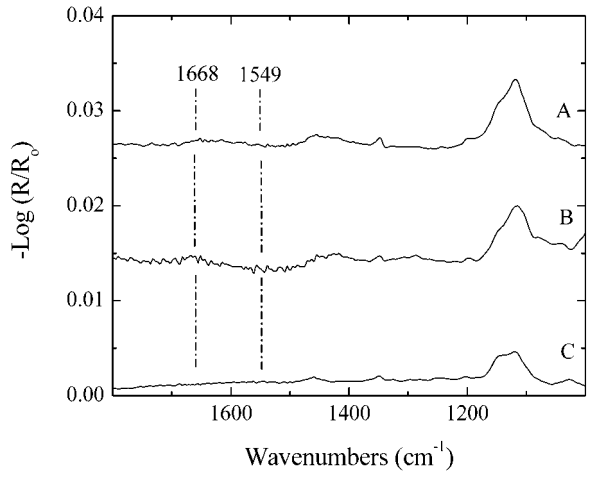

Figure 6. RAIRS spectra of the $HS(CH_2CH_2O)_6CH_3$ SAM from 1800 to 1000 cm^{-1} assembled from THF: spectrum A, before exposure to protein solutions; spectrum B, after exposure to BSA; spectrum C, after exposure to lysozyme. The spectra are offset for clarity.

amide II bands at ~1670 and ~1550 cm^{-1}, respectively.[35] The absence of bands in the 1700−1500 cm^{-1} region is evidence either that no protein adsorbed to these surfaces or that adsorbed protein was loosely bound to the surface and was removed by the subsequent washing step (see Experimental Section).

Figures 5−7 show that BSA adsorbed to the SAMs assembled from 95% ethanol only (spectrum B, Figure 5) whereas lysozyme adsorbed to the SAMs assembled from 95% and 100% ethanol (spectra C, Figures 5 and 7).[36] Importantly, these spectra also show that the A_2 bands in the 1400−1000 cm^{-1} region are nearly identical to those in the 1400−1000 cm^{-1} region before exposure to the protein solutions (spectra A), indicating that the underlying SAMs have not substantially changed from the ordered helix. On the other hand, neither protein (BSA or lysozyme) adsorbed to the SAMs assembled from THF (spectra B and C, respectively, Figure 6) nor did BSA adsorb to the SAMs assembled from 100% ethanol (spectrum B, Figure 7).[37] This second group of spectra show that the underlying SAMs were disordered or became disordered as indicated by the attenuation of the A_2 bands and/or the appearance of spectral features similar to those found for the SAMs from THF. In a control experiment, RAIRS data indicated that a SAM assembled from 95% ethanol was essentially unchanged after soaking in deionized water for 4 h (data not shown).

In one set of experiments, the $HS(CH_2CH_2O)_6CH_3$ SAMs were exposed to BSA and lysozyme for longer periods of time. The samples removed after 2 h were returned to the protein solutions for an additional 22 h. RAIRS data for these samples support the 2 h exposure results. The disordered SAMs remained protein resistant. For some SAMs, the presence of adsorbed protein was ambiguous because of poor water vapor subtraction resulting in an increase in RAIRS baseline noise in the 1700−1500 cm^{-1} region. The SAMs that remained largely in the helical conformation adsorbed more protein, relative to the 2 h exposure experiments, as indicated by a 2-fold increase in the intensities of the amide I and amide II bands.[36]

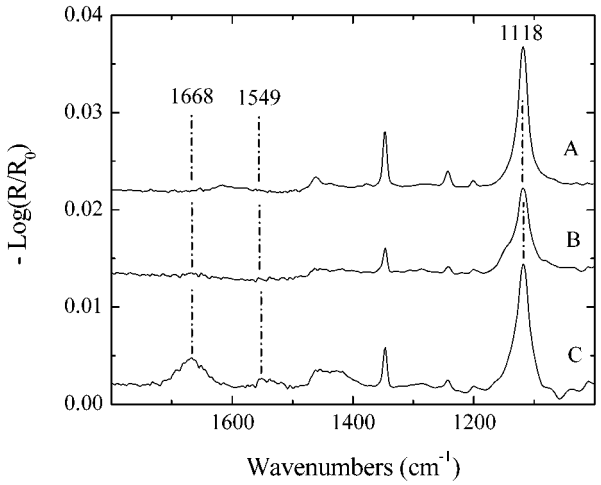

Figure 7. RAIRS spectra of the $HS(CH_2CH_2O)_6CH_3$ SAM from 1800 to 1000 cm^{-1} assembled from 100% ethanol: spectrum A, before exposure to protein solutions; spectrum B, after exposure to BSA; spectrum C, after exposure to lysozyme. The spectra are offset for clarity.

Discussion

We begin by discussing the structures of the SAMs from each solvent starting with the $HS(CH_2CH_2O)_6CH_3$ SAMs from 95% ethanol, which give a nearly perfect semicircular complex capacitance spectrum (spectrum C, Figure 1). As developed more fully elsewhere[38] (see Supporting Information), a perfect semicircular complex capacitance spectrum indicates a dielectric film that can be modeled as an equivalent circuit consisting of a series of R_sC

(35) Goormaghtigh, E.; de Jongh, H. H.; Ruysschaert, J.-M. *Appl. Spectrosc.* **1996**, *50*, 1519−1527.

(36) Estimated protein coverage (spectra B and C, Figure 5, and spectrum C, Figure 7) ≈ 50% of a monolayer from comparison of the intensities of amide I and amide II bands of BSA and lysozyme (~0.0032 au and ~0.0017 au, respectively) to those in ref 11 [amide $I_{fibrinogen}$ (~0.004 au) and amide $II_{fibrinogen}$ (~0.002 au) ≈ 60% of a protein monolayer], assuming all adsorbed proteins are essentially undenatured. The latter assumption is supported by near identical relative intensities of the BSA and lysozyme amide I/amide II bands (2/1) to those for fibrinogen (ref 11) and the known low denaturation of proteins on OEO chains (see: Yang, Z.; Galloway, J. A.; Yu, H. *Langmuir* **1999**, *15*, 8405). The ~50% coverage is further supported by the nearly 2 times absorbance of the amide I and amide II bands after 24 h [~0.006 au and ~0.003 au, respectively (data not shown)], from which a full protein monolayer is likely.

(37) The lower detectable limit is estimated at 2−3% of a protein monolayer.

(38) Vanderah, D. J.; Gates, R. S.; Silin, V.; Meuse, C. W.; Zeiger, D. N.; Valincius, G. *Langmuir*, submitted.

elements, where R_s is the electrolyte solution resistance and C is the capacitance of the interface. To account for surface heterogeneity of real electrochemical systems, capacitance is replaced by the constant phase element (CPE) characterized by its magnitude and exponent.[38] The CPE exponent for the SAMs from 95% ethanol was found to be 0.992 ± 0.004, indicating that these films behave as almost perfect capacitors. From the CPE magnitude ($3.39 \pm 0.30\ \mu F/cm^2$) and SE thickness ($1.96\ nm \pm 0.07\ nm$), we calculated a dielectric constant of ~7.2 which is similar to that found for the SAMs of $[S(CH_2CH_2O)_{6-8}C_{18}H_{37}]_2$ (5.36 ± 0.35[38]). This relatively low dielectric constant value indicates a homogeneous SAM with little or no water and/or ions present in the film. The RAIRS (spectra C, Figures 2 and 3) and SE data indicate that nearly all the OEO segments are in a 7/2 helical conformation. The structural model of a uniform film and, therefore, a more uniform film−air or film−solution interface is further supported by the contact angle data. Increasingly ordered, helical ω-OEO SAMs (R = CH_3), as illustrated in Figure 4 (also see pictures of molecular clusters in ref 20), should be more hydrophobic than their less ordered counterparts due to the ordered orientations of the methyl groups more effectively screening the underlying oxygen atoms in the OEO segments. The contact angle $\theta = 70° \pm 2°$ is significantly higher than that obtained previously ($\theta \approx 47°$) for the similar **1a** ($x = 6$, R = CH_3[14]) SAMs and is between the advancing and receding contact angles for SAMs of $HS(CH_2)_nOCH_3$, where $n = 6-16$.[39]

Increasingly ordered SAMs are also expected to be more robust due to OEO chain contact with nearest neighbors (lateral distance = 0.50 nm[20]), which leaves little room for nonhelical conformations or penetration by solvent. The near preclusion of solvent in highly ordered SAMs has been suggested in recent molecular modeling studies[12,21] and is supported in this work by the fact that the SAMs are resistant to disordering in pure water (4 h) and the presence of the ordered helical conformation after protein adsorption (Figures 5 and 7).

Consequently, we conclude the preparation of a robust, uniform, nearly all helical (i.e., single phase) ω-OEO SAM from 95% ethanol with imperfections below the detection limits of the RAIRS experiment and at or below the detection limits of the EIS experiment. The $HS(CH_2CH_2O)_6CH_3$ SAMs from this solvent are likely the most ordered OEO segments prepared thus far and are resistant to change or penetration by water or ions. We emphasize, however, that our data do not indicate perfect order and more ordered $HS(CH_2CH_2O)_6CH_3$, or other ω-OEO SAMs, could be obtained but likely will possess similar characteristics.

The $HS(CH_2CH_2O)_6CH_3$ SAMs from 100% ethanol give an EIS spectrum (spectrum B, Figure 1) that has a similar shape, CPE magnitude ($4.72 \pm 0.41\ \mu F/cm^2$), and CPE exponent ($0.989 \pm 0.002$) as compared to the spectrum of the SAMs from 95% ethanol. These data, coupled with the near identical RAIRS data (spectra B and C, Figures 2 and 3), indicate that the overall structure and electrical properties of the SAMs from 100% and 95% ethanol are similar. However, the EIS spectra of the SAMs from 100% and 95% ethanol exhibit subtle differences (spectra B and C, Figure 1 inset, respectively). As these data show, the real component of the complex capacitance [Re(Y/ω)] is nearly constant in spectrum C whereas it increases at low frequencies in spectrum B. The latter spectral feature indicates ionic conductivity in the SAMs which can be modeled by resistance parallel to the capacitance (or CPE)[38] and is indicative of pinholes and/or collapse sites.

The factors causing the differences in the SAMs from the ethanolic solvents are not obvious and are currently under investigation. As argued earlier,[11,19,20] a tightly bound water film at the top of the OEO segments is possible. The availability of water during SAM formation from 95% ethanol would make the formation of such a water film more likely. While we present no direct evidence for the presence or absence of such associated water, it is conceivable that a water film at the top of the OEO segment might stabilize the SAMs in the helical conformation resulting in a SAM from 95% ethanol that is more insulating. Alternatively, the differences may be the result of slightly different kinetics of SAM formation. Whatever the cause, the SAMs from 100% ethanol appear to be less robust in the presence of an aqueous environment, as may be also inferred from the subsequent protein adsorption discussion.

The EIS, RAIRS, SE, and contact angle data indicate that the $HS(CH_2CH_2O)_6CH_3$ SAMs assembled from THF are significantly less ordered and less densely packed. The RAIRS data (spectra A, Figures 2 and 3) clearly indicate less ordered OEO segments consisting of both helical and nonhelical conformations. The SAMs from THF have higher CPE magnitude (7.93 ± 1.73) and lower CPE exponent ($0.975 \pm 0.004\ \mu F/cm^2$) values indicative of greater film irregularities, relative to the SAMs from the ethanolic solvents, and suggest the presence of more defects (pinholes/collapse sites) and water/ions in these films.

Exposure of the different $HS(CH_2CH_2O)_6CH_3$ SAMs to BSA and lysozyme establishes a correlation between ω-OEO SAM order on gold and protein resistance. BSA and lysozyme adsorb to the most ordered, helical $HS(CH_2CH_2O)_6CH_3$ SAMs, from 95% ethanol (Figure 5), and do not adsorb to the disordered $HS(CH_2CH_2O)_6CH_3$ SAMs, from THF (Figure 6). These data establish, for the first time, the difference between a protein-adsorbent surface [ordered, nearly homogeneous helical conformation, symmetrical A_2 (6) band] and a protein-resistant surface [less ordered, mixture of helical and nonhelical conformations, asymmetrical A_2 (6) band] with the same compound on the same substrate.

Although the complete mechanism is unclear, the protein resistance/ω-OEO SAM order correlation is further illustrated by the BSA data for the SAMs assembled from 95% ethanol and 100% ethanol (spectra B, Figures 5 and 7, respectively). On close inspection, these spectra show that both SAMs exhibit increased disorder after exposure to BSA solutions. Of the two, the SAMs assembled from 100% ethanol became more disordered, as indicated by the significant ~1140 cm^{-1} shoulder on the 1118 cm^{-1} band. These $HS(CH_2CH_2O)_6CH_3$ SAMs did not adsorb BSA. A similar disordering of SAMs in contact with protein solutions and a concurrent decrease in protein adsorption have been reported.[11] On the other hand, the SAMs from 95% ethanol are only slightly disordered, as indicated by only a slightly greater fwhm of the 1118 cm^{-1} band. These minimally disordered $HS(CH_2CH_2O)_6CH_3$ SAMs adsorbed BSA. Thus, while the data on the SAMs from 95% ethanol and THF define the difference between protein adsorbent and protein resistant over a relatively large range in SAM order, the BSA data on the SAMs from 95% and 100% ethanol specify this difference within a much smaller range in SAM order.

The SAMs assembled from 95% ethanol appear to be more resistant to the disordering effects of the BSA solutions than are the SAMs assembled from 100% ethanol

(39) Laibinis, P. E.; Bain, C. D.; Nuzzo, R. G.; Whitesides, G. M. *J. Phys. Chem.* **1995**, *99*, 7663−7676.

(spectra B, Figures 5 and 7). The $HS(CH_2CH_2O)_6CH_3$ SAMs from 100% ethanol, with less order and/or increased defect sites, may be more susceptible to protein−SAM interactions which could lead to further SAM disordering. We hypothesize that the SAM changes (disordering) during exposure to protein solutions are due to BSA[40] and not to the water or buffer salts because all protein solutions contained the same buffer salts, the helix readily forms in the presence of ~5% water, and the ordered $HS(CH_2CH_2O)_6CH_3$ SAMs showed little or no increase in disorder in the presence of water for extended periods (4 h).

Our protein adsorption results do not offer closure to the question, is it the conformational freedom of the OEO segment or the presence of water (ions?[9]) in the SAMs that imparts fouling (protein) resistance? On one hand, the protein resistance of the $HS(CH_2CH_2O)_6CH_3$ SAMs from THF, with lower packing densities, would be expected to be more flexible, thus supporting the "steric repulsion" model.[41] On the other hand, the lower packing densities would also allow water to more easily penetrate down the OEO segments promoting more significant layers of bound water,[20] thus consistent with the water repulsion (osmotic) theory.

Conclusions

The conformational composition and order of the SAMs of $HS(CH_2CH_2O)_6CH_3$ on Au were found to depend on the solvent from which the films were formed. For samples assembled from 95% or 100% ethanol, EIS, RAIRS, and SE data indicate highly uniform SAMs in which the OEO segments, oriented normal to the substrate, adopt the folded-chain crystal structure of crystalline PEO, that is, a well-ordered 7/2 helical conformation. EIS data, however, reveal that the SAMs from these two solvents are slightly different with the latter being slightly less insulating. In contrast, for samples assembled from THF over the same period, the EIS, RAIRS, and SE data indicate that less ordered SAMs are obtained. These disordered SAMs consist of OEO segments that are mixtures of helical and nonhelical conformations. Exposure of these ordered and disordered $HS(CH_2CH_2O)_6CH_3$ SAMs to BSA or lysozyme solutions resulted in protein adsorption to the SAMs in the ordered helical conformation and inhibition of protein adsorption by all SAMs which contained a significant component of nonhelical conformations.

Acknowledgment. The authors express their appreciation to Dr. Ken Rubinson and Professor Hyuk Yu for helpful discussions, Dr. Vitalii Silin for the preparation of the gold substrates, and the NIST Advanced Technology Program for financial support.

Supporting Information Available: Details of modeling a dielectric film as an equivalent circuit. This material is available free of charge via the Internet at http://pubs.acs.org.

LA025720T

(40) Our preliminary data suggesting protein-induced conformational changes in the SAMs are consistent with earlier data (ref 11) but will require a more systematic study to determine the validity of this hypothesis and to define the scope and magnitude of such effects.

(41) Morra, M. *J. Biomater. Sci., Polym. Ed.* **2000**, *11*, 547−569.